National Metrology Institute VTT MIKES
December 4, 2025

Frequency evaluation of MIKES AHM3 by MIKES-Sr+1 for the period MJD 60579 to 60614

The frequency of the hydrogen maser (HM) MIKES AHM3 (1404189) was evaluated during the 35-day period MJD 60579 to 60614 using the $^{88}Sr^+$ optical single-ion frequency standard MIKES-Sr+1 (1784101) and an optical frequency comb. The $^{88}Sr^+$ standard operated for 88.6% of the period. The evaluation is based on the 2021 recommended frequency for the $5s\,^2S_{1/2} \rightarrow 4d\,^2D_{5/2}$ transition in $^{88}Sr^+$, 444 779 044 095 486.3 Hz, with a fractional uncertainty of 1.3×10^{-15} [1]. The results of the evaluation are given in Table 1. The operation and uncertainty evaluation of MIKES-Sr+1 are described in [2] and summarized below.

Table 1: Results of the evaluation of AHM3 by MIKES-Sr+1.

Period of estimation	y(AHM3/Sr+1) $/10^{-15}$	u_A $/10^{-15}$	u_B $/10^{-15}$	$u_{A/Lab}$ $/10^{-15}$	$u_{B/Lab}$ $/10^{-15}$	u_{Srep} $/10^{-15}$	Uptime %
60579–60614	−2313.51	0.0024	0.0039	0.096	0.020	1.3	88.6

1 Measurement configuration

The measurement configuration is schematically shown in Fig. 1. The clock laser is a 1348 nm external-cavity diode laser (ECDL), which is frequency-doubled to 674 nm and stabilized to a 30 cm ultra-low-expansion (ULE) glass cavity. The light to the ion and the frequency comb is de-drifted by an acousto-optic modulator (AOM, frequency f_{drift}) based on feedback from the ion. Using another AOM (frequency f_{Zeeman}), independent servo loops track six Zeeman components of the clock transition, whose mean is free from linear Zeeman shift and tensor shifts. The fibre frequency comb is optically locked to the clock laser. The frequency ratio between the HM and MIKES-Sr+1 is determined from the AOM frequencies, the in-loop beat note between the clock

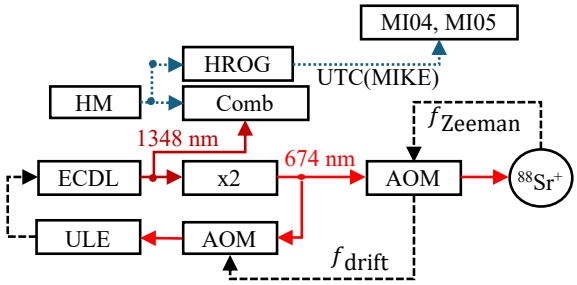

Figure 1: Clock-laser setup and frequency chain to the $^{88}Sr^+$ ion, frequency comb, hydrogen maser (HM), and geodetic GNSS receivers MI04 and MI05 for time transfer. HROG—high resolution offset generator. Solid (dotted) lines indicate optical (rf) signals, while dashed lines indicate feedback loops for Pound-Drever-Hall locking (left), drift compensation of the cavity (f_{drift}, middle), and tracking the Zeeman components of the clock transition (f_{Zeeman}, right). AOMs for fiber noise cancellation are not shown. Adapted from [2].

laser and the comb, and from the comb repetition rate and carrier offset frequency measured against the HM. For details, see [2].

2 MIKES-Sr+1 evaluation

A detailed uncertainty evaluation is presented in [2]. The statistical uncertainty $u_{\mathrm{A},i}$ of a particular measurement i is estimated from a $\tau^{-1/2}$ fit to the clock self-comparison instability evaluated at the total measurement time τ_i (including valid data only). The instability is typically around $2.5 \times 10^{-15}\tau^{-1/2}$, where τ is in seconds, but varies with the probe time (and dead time). During this evaluation period, it was on average $3.7{\times}10^{-15}\tau^{-1/2}$. The higher instability was due to a few measurements without state preparation (spin polarization) due to a different bias field direction being used and due to interleaved measurements used for the polarizability evaluation in [4]. Here, only the unperturbed reference servo data was used, which increased the effective deadtime to >50 %. The total u_{A} of the period is determined as $u_{\mathrm{A}} = (\sum_i w_i^2 u_{\mathrm{A},i}^2)^{1/2}$, where the weights are proportional to the duration of the individual measurements, $w_i = \tau_i/(\sum_i \tau_i)$.

Several systematic frequency shifts are evaluated dynamically. Also several systematic uncertainty contributions j depend on parameters such as the probe time (light shifts, thermal motion shifts via the ion heating rate), the Zeeman AOM rf power (AOM chirp), the trap drive voltage (blackbody radiation shift), and the electric quadrupole shift and excess micromotion measured during a clock run. Each uncertainty contribution is assumed to be fully correlated throughout the evaluation period so that its weighted mean is $u_{\mathrm{B},j} = \sum_i w_i u_{\mathrm{B},i,j}$. The total systematic uncertainty is then evaluated as $u_{\mathrm{B}} = (\sum_j u_{\mathrm{B},j}^2)^{1/2}$.*

Due to the Fennoscandian land uplift (postglacial rebound), the height of the clock relative to the reference potential $W_0 = 62\,636\,856.00\,\mathrm{m}^2/\mathrm{s}^2$ increases by 3.8 mm/y. For simplicity, this evaluation has been automated based on the mean epoch of a particular measurement. The uncertainty of the gravitational redshift, 2.4×10^{-18}, is added in quadrature to that of the clock itself. Tidal effects are neglected due to our high uptime and because the amplitude of solid Earth tides decreases with increasing latitude [3] (MIKES's latitude is 60.2°).

A mean uncertainty budget for the evaluation period is shown in Table 2. Note that we use the differential static scalar polarizability $\Delta\alpha_0$ from [4].

3 Frequency comparison

The measured maser frequency and the uptime of MIKES-Sr+1 for the evaluation period are shown in Fig. 2. The statistical uncertainty $u_{\mathrm{A/Lab}}$ includes the uncertainty due to the dead time of MIKES-Sr+1 (DTU). The DTU consists of a deterministic part due to the HM drift and a stochastic part. The HM drift is very linear, but, in addition, the HM frequency undergoes random frequency jumps between two "levels" [2]. To separate the deterministic drift from the stochastic frequency jumps, we evaluate the drift from a linear fit to the full 10 month period 2024-06–2025-03. The frequency at the middle of the evaluation period is obtained by correcting the measured mean frequency using the drift and the offset between the middle point and the barycenter of the data. The noise model for the maser is presented in Appendix E of [2] and is summarized in Table 3. As in [5], the bump in the PSD caused by the quasi-periodic frequency jumps is described by a Lorentzian peak. The extrapolation uncertainty is evaluated using the Fourier transform method [6].

The UTC(k)-HM data is submitted to the BIPM with a resolution of 0.1 ns. The standard deviation of the rectangular distribution of rounding errors is $u_x = 0.1/\sqrt{12}$ ns. When evaluating

*Note that in [2], the total uncertainty was evaluated as a weighted mean of the total uncertainty of each measurement, $u_{\mathrm{B}} = \sum_i w_i u_{\mathrm{B},i}$, which gave slightly larger uncertainties for months with significantly varying systematics. However, the systematic uncertainty of the clock is in any case negligible compared to the other contributions related to TAI calibration or absolute frequency measurements.

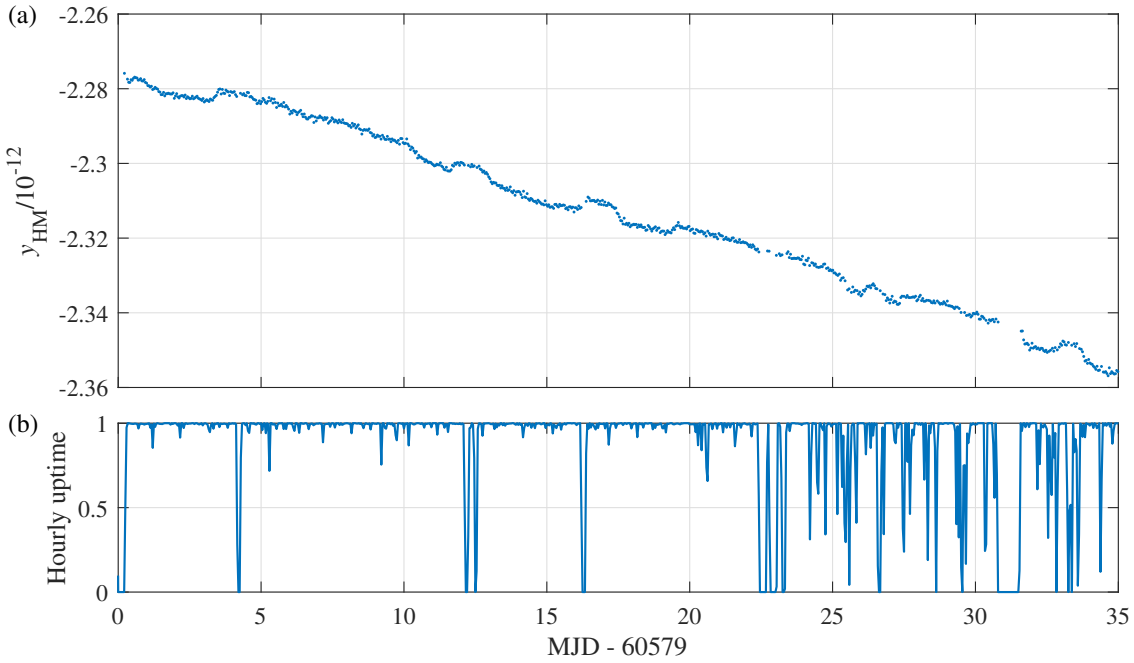

Figure 2: (a) Maser fractional frequency as measured against MIKES-Sr+1 in 3600 s bins and (b) hourly uptime of MIKES-Sr+1 over the evaluation period (total uptime 88.6%).

the mean frequency over a period of duration T, this gives rise to a fractional uncertainty $u_y = \sqrt{2}u_x/T \approx 4.7 \times 10^{-16}/(T/\mathrm{d})$. The uncertainty of the measurement itself is negligible in comparison. The UTC(k)-HM uncertainty is included in $u_{\mathrm{A/Lab}}$.

An upper limit of 2×10^{-17} for the systematic uncertainty $u_{\mathrm{B/Lab}}$ was estimated in a comparison between two frequency combs with independent rf distribution [2]. The corresponding statistical uncertainty was found to be negligible compared to $u_{\mathrm{B/Lab}}$ for relevant measurement times and is not included in $u_{\mathrm{A/Lab}}$. The $u_{\mathrm{A/Lab}}$ and $u_{\mathrm{B/Lab}}$ contributions are summarized in Table 4.

References

[1] H. S. Margolis *et al.*, The CIPM list 'Recommended values of standard frequencies': 2021 update, Metrologia **61**, 035005 (2024).

[2] T. Lindvall *et al.*, $^{88}Sr^+$ optical clock with 7.9×10^{-19} systematic uncertainty and its absolute frequency with 9.8×10^{-17} uncertainty, Phys. Rev. Applied **24**, 044082 (2025).

[3] C. Voigt *et al.*, Time-variable gravity potential components for optical clock comparisons and the definition of international time scales, Metrologia **63**, 1365 (2016).

[4] T. Lindvall *et al.*, Measurement of the Differential Static Scalar Polarizability of the $^{88}Sr^+$ Clock Transition, Phys. Rev. Lett. **135**, 043402 (2025).

[5] T. Lindvall *et al.*, Coordinated international comparisons between optical clocks connected via fiber and satellite links, Optica **12**, 843–852 (2025).

[6] S. T. Dawkins *et al.*, Considerations on the measurement of the stability of oscillators with frequency counters, IEEE Trans. Ultrason., Ferroelectr., Freq. Control **54**, 918 (2007).

Table 2: Uncertainty budget for MIKES-Sr+1 for the reported evaluation period (10^{-18}).

Contribution	Shift	Uncertainty
Blackbody radiation (BBR) E1 shift	525.99	
BBR field		0.30
Differential polarizability $\Delta\alpha_0^{\dagger}$		0.22
Dynamic correction η		0.090
BBR M1 shift	−0.010 20	0.000 20
Collisional shift	0.00	0.22
Thermal motion shifts	−2.04	0.81
Electrical quadrupole shift	0.0	2.9‡
Excess micromotion shifts	0.000	0.013
Tensor Stark shift	0.000 00	0.000 92
674 nm E1 ac Stark shift	0.0065	0.0065
674 nm E2 ac Stark shift	0.000	0.015
Quadratic Zeeman shift, static field	0.1603	0.0031
AOM chirp	0.00	0.29
Servo errors	0.00	0.10
First-order Doppler shifts	0.00	0.50
Total, Sr^+	524.1	3.1
Gravitational redshift	803.0	2.4
Total	1327.1	3.9

† $\Delta\alpha_0 = -4.8314(20) \times 10^{-40}\mathrm{Jm}^2/\mathrm{V}^2$ [4].
‡ Larger than normal due to characterization measurements with deliberately applied high electric quadrupole shift.

Table 3: Maser noise coefficients for the one-sided fractional-frequency power-spectral-density (PSD) model, $S_y(f) = h_2 f^2 + h_0 + h_{-1}/f + A/[1 + (f - f_0)^2/\delta f^2]$. The coefficients for the polynomial-law noise types h_i are given as ADEV at 1 s and converted to fractional-frequency PSD S_y. From [2].

White phase noise	h_2	$(4.0 \times 10^{-13})^2/(0.076/2)$	Hz^{-3}
White frequency noise	h_0	$2(2.5 \times 10^{-14})^2$	Hz^{-1}
Flicker frequency noise	h_{-1}	$(0.5 \times 10^{-16})^2/(2\ln 2)$	1
Lorentzian peak	A	6.5×10^{-24}	Hz^{-1}
	f_0	5×10^{-8}	Hz
	δf	0.55×10^{-6}	Hz

Table 4: Contributions to $u_{\mathrm{A/Lab}}$ and $u_{\mathrm{B/Lab}}$.

Contribution	Uncertainty/10^{-15}
Extrapolation (stochastic)	0.095
Extrapolation (drift)	0.0001
UTC(MIKE)-HM rounding	0.014
$u_{\mathrm{A/Lab}}$ total	0.096
rf distribution/synthesis	0.020
$u_{\mathrm{B/Lab}}$ total	0.020